Surface Engineering

ISSN: 0267-0844 (Print) 1743-2944 (Online) Journal homepage: https://www.tandfonline.com/loi/ysue20

Influence of annealing temperature on ζ-$CrZn_{13}$ formation in electrodeposited Zn–Cr coatings

Tzvetanka Boiadjieva-Scherzer, Georgi Avdeev, Tsvetan Vassilev, Vesselina Chakarova, Hermann Kronberger & Milko Monev

To cite this article: Tzvetanka Boiadjieva-Scherzer, Georgi Avdeev, Tsvetan Vassilev, Vesselina Chakarova, Hermann Kronberger & Milko Monev (2019): Influence of annealing temperature on ζ-$CrZn_{13}$ formation in electrodeposited Zn–Cr coatings, Surface Engineering, DOI: 10.1080/02670844.2019.1598023

To link to this article: https://doi.org/10.1080/02670844.2019.1598023

Published online: 01 Apr 2019.

SURFACE ENGINEERING
https://doi.org/10.1080/02670844.2019.1598023

The Institute of Materials, Minerals and Mining

Taylor & Francis
Taylor & Francis Group

Influence of annealing temperature on ζ-$CrZn_{13}$ formation in electrodeposited Zn–Cr coatings

Tzvetanka Boiadjieva-Scherzer[a], Georgi Avdeev[b], Tsvetan Vassilev[b], Vesselina Chakarova[b], Hermann Kronberger[c] and Milko Monev[b]

[a]Centre of Electrochemical Surface Technology GmbH (CEST), Wiener Neustadt, Austria; [b]Institute of Physical Chemistry, Bulgarian Academy of Sciences, Sofia, Bulgaria; [c]Institute of Chemical Technologies and Analytics, Technical University of Vienna, Vienna, Austria

ABSTRACT

Electrodeposited Zn–Cr alloy coatings, containing 3.6, 5.4 and 9.4 mass % Cr were analysed by DSC and XRD. X-ray diffraction patterns of the samples show that when they are annealed to selected temperatures before and after the heat flow peaks of the DSC curve, there is an irreversible transition in all three alloys from η-(Zn, Cr) to ζ-$CrZn_{13}$ phase. With increasing Cr content, the start of the transition is shifted to higher temperatures (from 180 to 250°C). The η-(Zn) phase is predominant in the annealed alloy with the lowest content of Cr. In the case of the alloy with the highest Cr content, typical XRD lines of Cr appear along with those of the ζ-$CrZn_{13}$ phase. The Zn–Cr coating containing 5.4 mass % Cr transforms almost completely into ζ-$CrZn_{13}$ phase with insignificant traces of residual initial η-(Zn, Cr) phase.

ARTICLE HISTORY
Received 13 September 2018
Revised 15 February 2019
Accepted 12 March 2019

KEYWORDS
Electrodeposition; Zn–Cr alloy coatings; annealing; phase composition; phase transition; DSC; XRD

Introduction

Zn–Cr alloy coatings are of interest due to their better corrosion-protective properties than zinc coatings even at low thicknesses. The process of electrodeposition of Zn–Cr has been optimised over the years to enable high-speed deposition on steel strips for car body panels in the automotive industry [1,2].

The protective properties of Zn–Cr alloys have been attributed by some researchers to their phase composition. Solid Cr has poor solubility in liquid Zn, which makes it difficult to obtain even low-Cr alloys [3]. For this reason, the Cr–Zn equilibrium phase diagram has been evaluated for Zn-rich alloys, where two inter-metallic compounds – θ-$CrZn_{17}$ [4] and ζ-$CrZn_{13}$ [5] have been reported. Brown suggested that ζ-$CrZn_{13}$ is probably isotypic with several ζ-MZn_{13} (M = Co, Fe, Mn) phases [6].

Unlike conventional alloys, several non-equilibrium Zn–Cr phases have been found in Zn–Cr coatings that have been produced by electrodeposition [7] and physical vapour deposition [8]. Upon increasing the Cr content in the alloy, the phase composition of the coatings changes in the following sequence: hexagonal η-(Zn, Cr) → hexagonal δ-(Zn, Cr) → cubic Γ-(Zn, Cr), including concentration intervals in which two or all three phases co-exist [7–10]. When annealed at relatively low temperatures (170–225°C), the δ-phase in vapour deposited coatings transforms to a mixture of phases (ζ+δ) or to a single phase (ζ), depending on the temperature and Cr content, while the Γ-phase is stable up to at least 275°C [9]. Irreversible transition of δ- and Γ-super-saturated solid solutions to ζ-$CrZn_{13}$ phase is also found in electrodeposited alloys [11,12]. Despite the complexity in phases, investigations on these alloys have not been systematic. In our previous studies, the electrodeposited samples were annealed only at 260°C [12] at which, the transformation of the Γ- phase into ζ-$CrZn_{13}$ phase was already established, unlike the case of evaporated layers.

In a previous work, the corrosion protection properties of 'as electrodeposited' Zn–Cr alloy coatings with different amounts of chromium were studied [13]. In the present work, the influence of annealing temperature on the phase transformation in electrodeposited alloys is investigated. The aim is to establish the conditions for producing a coating containing ζ-$CrZn_{13}$ phase. Such a coating can be further investigated for its corrosion-protective and electrochemical behaviour, on which no data are currently available.

Experimental

Zn–Cr alloy coatings were electrodeposited from an electrolyte, containing 40 g L^{-1} Zn, 15 g l^{-1} Cr (both added as sulphates) and PEG 6000 (1 g L^{-1}). The pH was kept at 2.0 with sulphuric acid, and the electrodeposition was performed in a 20 L flow cell, at an electrolyte flow rate 4 m s^{-1}, with electrolyte temperature of 40°C. The alloys were electrodeposited onto mild steel substrates, in mass %: C-0.12, Mn-0.6, P-0.045,

CONTACT Tzvetanka Boiadjieva-Scherzer tzvetanka.boiadjieva@cest.at Centre of Electrochemical Surface Technology GmbH (CEST), Wiener Neustadt A, 2700, Austria

S-0.045 (Metall-Folien GmbH, Main, Germany) and of dimensions 115 × 85 mm. For further analyses, samples of appropriate sizes were cut. At a current density of 80 A dm^{-2}, alloy coatings with an average Cr content of 3.6 mass % and average thickness of 5 μm were obtained after 22 s of electrodeposition. When the current density was 90 A dm^{-2}, Zn-5.4%Cr coatings were deposited with an average thickness of 5 μm at 18 s of electrodeposition. Zn-9.4%Cr coatings with an average thickness of 5 μm were deposited when the current density was 120 A dm^{-2} and electrodeposition performed for 14 s.

The Cr content in the alloy coatings as well as the coatings thickness was determined using X-ray fluorescence analysis (XRFA) (Fischerscope XDL-B, Software WinFTM 6.09). The elemental composition was measured by Energy Dispersive X-Ray (EDX) spectrometer supported with Genesis software (USA).

Differential scanning calorimetric experiments (DSC) were performed using DDSC7 (PE Instruments with PYRIS software). Temperature calibration was performed using In, Sn and Zn metals with purity higher than 99%. The heat of fusion of In was used to calibrate heat flow signal of the instrument and was checked using heat capacity calibration across the entire temperature range with sapphire disc as a standard. Baselines with empty pans were always measured before every experiment and they were subtracted from the recorded curves to correct for possible curvature. Samples were cut from the galvanised sheets in the form of a disc. Dry nitrogen flowing at a rate of 25 mL min^{-1} was used as purge gas. The samples were annealed between 30 and 400°C with a constant heating/cooling rate of 10 K min^{-1}.

For phase identification, X-ray powder diffraction patterns of 'as deposited' coatings annealed to selected temperatures were recorded in the angle interval 35–115° (2θ) using Philips PW 1050 diffractometer, equipped with CuK_α tube and scintillation detector. Data for Rietveld refinements were collected in θ–2θ, step-scan mode in the angle interval from 35 to 115° (2θ), at steps of 0.03° (2θ) and counting times of 3 s/step. Indexing, determination of unit cell parameters and evaluation of volume fraction of phase constituents were carried out using least-squares procedure of profile fitting, performed using the PowderCell software package [14]. As a structural analogue for all the solid solutions the structure of equilibrium Zn was used (Cross-References: ICSD:653502, ICDD:98-065-3502). For identification of the $CrZn_{13}$ compound, the structural analogue with Mn was utilised (Cross-References: ICSD:105023, ICDD:03-065-1239, ICDD:98-010-5023).

The modification of surface morphology as a result of the thermal impact was observed by scanning electron microscopy (SEM) (JSM 5300, Jeol, Japan).

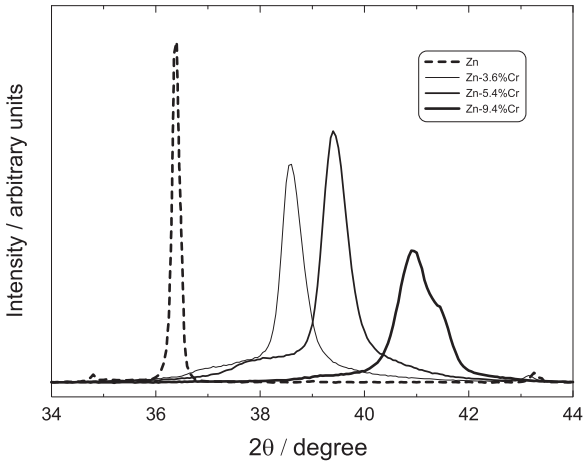

Figure 1. XRD patterns of Zn and 'as deposited' Zn–Cr alloy coatings with a different content of Cr.

Results

Phase composition of 'as deposited' Zn–Cr alloy coatings

Typical XRD patterns for the 'as deposited' Zn–Cr alloy coatings with different amounts of Cr are presented in Figure 1. The 'as prepared' alloy coatings consist of non-equilibrium Zn–Cr phase with lattice parameters within the boundaries 2.553(5) Å < a < 2.674(3) Å and 4.560(3) Å < c < 4.803(4) Å. With an increase in Cr content, the parameters of the lattice decrease in a regular way (Table 1). Some authors define solid solutions that contain up to 15 mass % of Cr as having the following lattice parameters: a = 2.66–2.74 Å and c = 4.61–4.95 Å as η-(Zn, Cr) phase (super-saturated solid solution of Cr in Zn matrix) [7]. Limited solid solutions of Cr in Zn with a hexagonal lattice, a = 2.72–2.78 Å and c = 4.43–4.60 Å have been denoted as δ- (Zn, Cr) phase [7]. In the present study, the unit cell parameters are closer to those of a hexagonal lattice characteristic for η-(Zn), and therefore will be referred to η-(Zn, Cr).

Table 1. Phase composition and unit cell parameters for 'as deposited' Zn and Zn–Cr alloy coatings.

Sample	Phase composition	Cell parameters (Å)	Volume (A^3)	c/a
Zn	η-Zn	a = 2.676(2) c = 4.965(3)	30.79	1.855
Zn–3.6%Cr	η-(Zn,Cr)	a = 2.674(3) c = 4.803(4)	29.74	1.796
Zn–5.4%Cr	η-(Zn,Cr)	a = 2.628(3) c = 4.734(2)	28.32	1.801
Zn–9.4%Cr	η-(Zn,Cr)	a = 2.553(5) c = 4.560(3)	25.74	1.786

The coatings are relatively thin, so that the XRD patterns also contain lines of α-Fe (body-centred cubic (bcc) lattice) due to diffraction from the substrate.

DSC and XRD investigation of Zn and Zn–Cr alloy coatings with a different content of Cr

Initially, the samples were annealed to 400°C. The DSC curves show thermal effects, which could be related to a reorganisation of the alloy coating. No peaks or other special features are observed on all cooling curves, which means that the transformations are irreversible with respect to temperature. Thereafter, a calorimeter was used under the same conditions as the oven-based annealing, to heat the samples to selected temperature before and after the heat flow peaks. Subsequently, X-ray powder diffraction patterns were obtained from the heated samples.

Figure 2 presents the relationships in the sample with alloy coating Zn–3.6%Cr. The inset in Figure 2 shows the part of the DSC curve with the peak, which is specific for this alloy in the temperature range of 180–230°C. The diffractograms of the alloy coating, annealed in this temperature range show that a process of transition of the η-(Zn, Cr) phase to ζ-$CrZn_{13}$ phase begins at a temperature of 180°C. This process ends at 230°C ($a = 10.864(3)$ Å, $b = 7.649(3)$ Å, $c = 5.199(1)$ Å; $\beta = 101.432(3)$ Å). The average content of Cr in the alloy is approximately two times lower than that of ζ-$CrZn_{13}$. Thus, a significant amount of η-(Zn) remains in the layer. Figure 3 presents the relationships, observed with the sample of alloy coating Zn–5.4%Cr. After annealing to a temperature of 180°C, the alloy coating Zn–5.4%Cr largely contains ζ-$CrZn_{13}$ ($a = 11.007(3)$ Å, $b = 7.622(3)$ Å, $c = 5.186(2)$ Å; $\beta = 100.514(6)$ Å). Traces of η-(Zn) phase are also seen, since the average content of Cr into the alloy is slightly lower than the stoichiometric content for the phase ζ-$CrZn_{13}$. This picture remains unchanged at 230°C. The analyses of the sample with a coating containing 9.4 mass % Cr

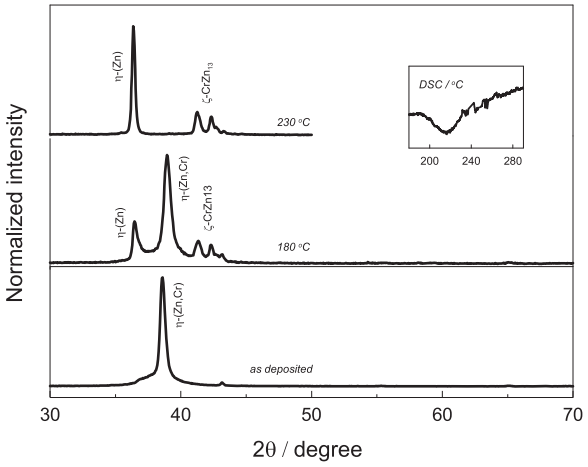

Figure 2. XRD patterns of 'as deposited' and annealed to different temperatures Zn–3.6%Cr alloy coating.

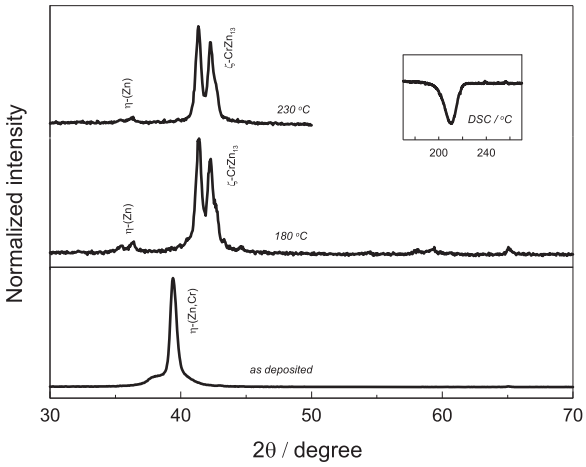

Figure 3. XRD patterns of 'as deposited' and annealed to different temperatures Zn–5.4%Cr alloy coating.

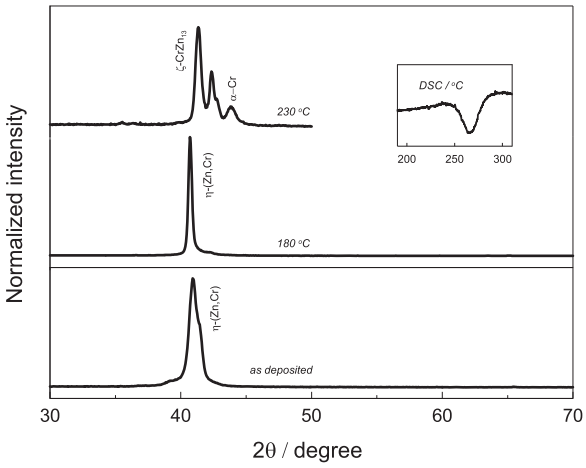

Figure 4. XRD patterns for 'as deposited' and annealed to different temperatures Zn–9.4%Cr alloy coating.

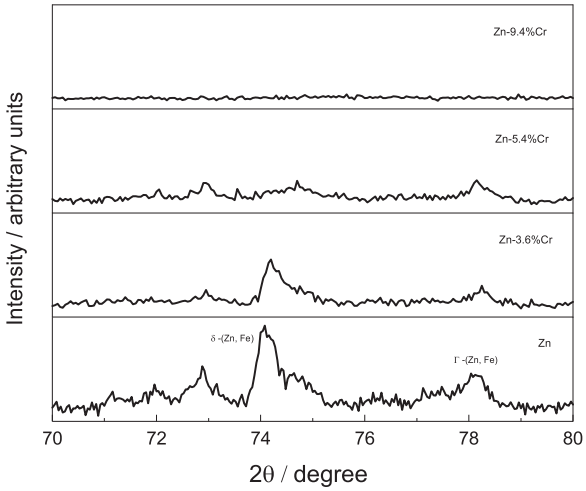

Figure 5. XRD patterns in the angular range 70–80° of Zn coatings and Zn–Cr alloy coatings with a different content of Cr after their annealing to 400°C.

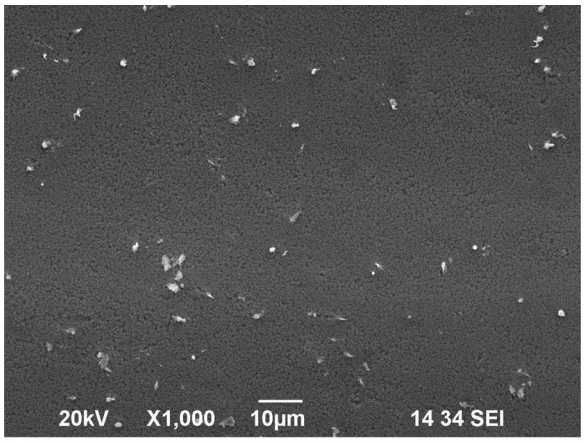

a

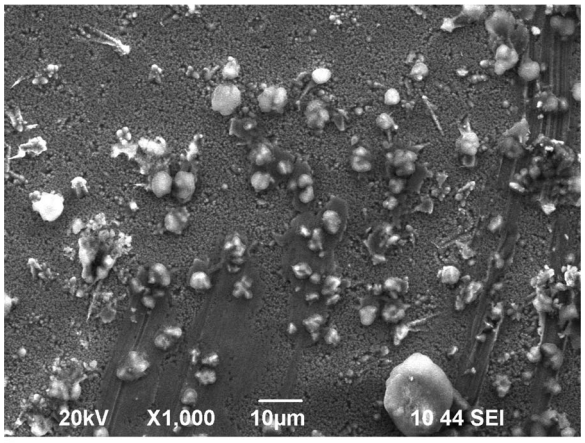

b

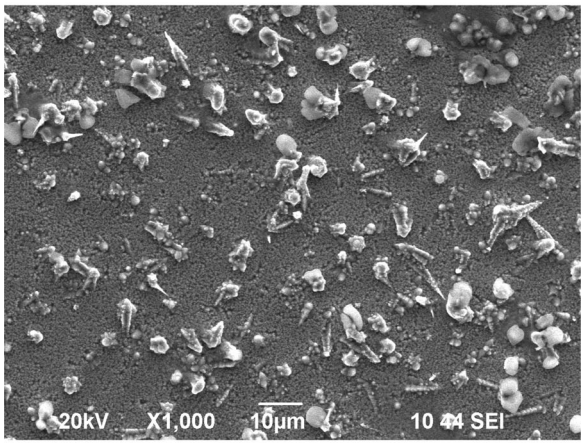

c

Figure 6. SEM of alloy coating Zn–Cr with 3.6 mass % Cr 'as deposited' (a) and after annealing at 180°C (b) or at 230°C (c).

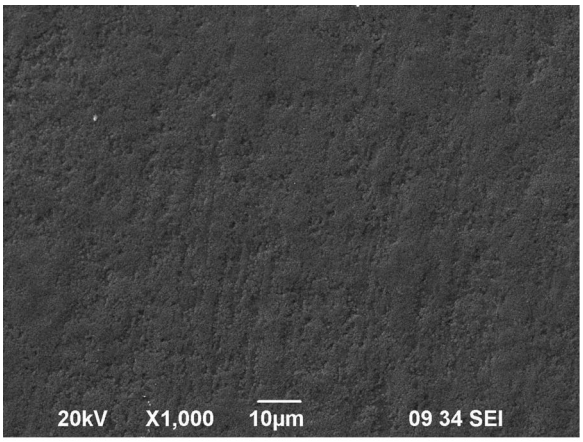

a

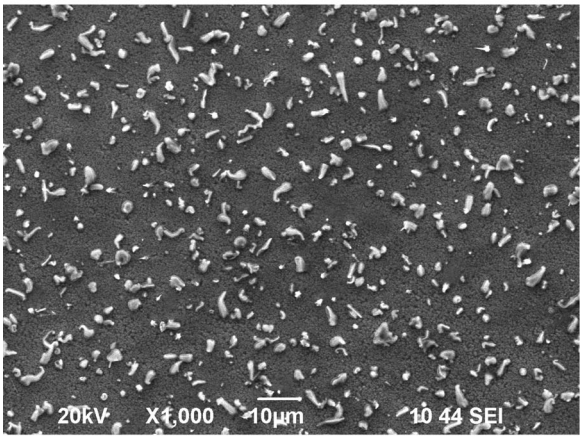

b

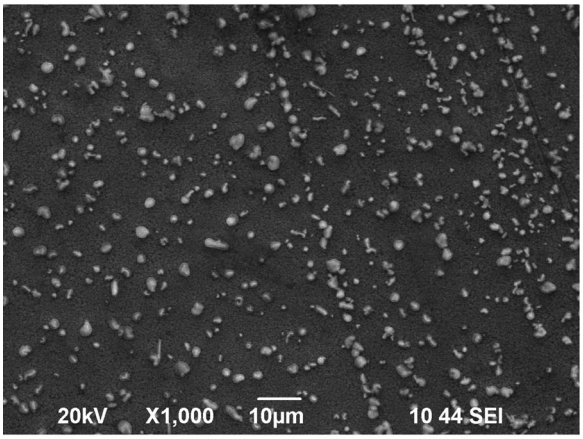

c

Figure 7. SEM of the alloy coating Zn–Cr with 5.4 mass % Cr 'as deposited' (a) and after annealing at 180°C (b) or at 230°C (c).

show that the transition occurs at a higher temperature range of 245–290°C (Figure 4, inset) ($a = 11.031$ (1) Å, $b = 7.699(1)$ Å, $c = 5.1985(7)$ Å; $\beta = 101.420$ (2)°). In this case, a peak appears at about 43.8°, corresponding to α-Cr phase. The values of the parameters of the ζ-$CrZn_{13}$ phase for the alloy coatings are close to each other. They are also close to the corresponding values registered by other authors [9,11] as well as in our previous studies [12].

The exothermic peaks of the DSC curves at temperatures higher than 300°C also deserve attention. Peaks are observed in the cases of Zn coating and alloy coating with 3.6 mass % Cr, and can be related to interaction with the substrate. Such peaks are not seen in samples with higher content of Cr. These assumptions are confirmed by the X-ray spectra of Zn coating and alloy coatings Zn–Cr with different amounts of Cr, after annealing to 400°C (Figure 5). The spectra are located in the angular range, characteristic for Zn–Fe alloys which are formed by annealing of galvanised steel [15]. In the case of Zn coating, two

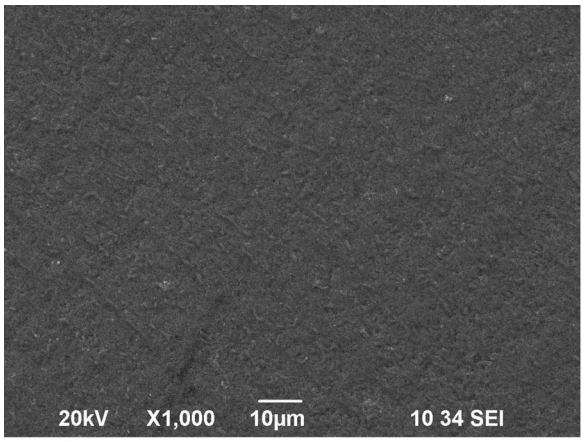

a

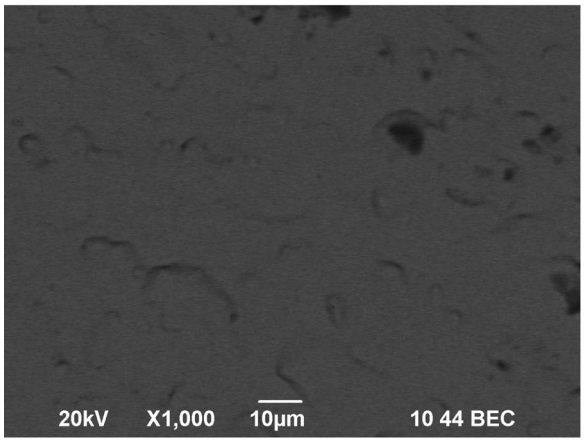

b

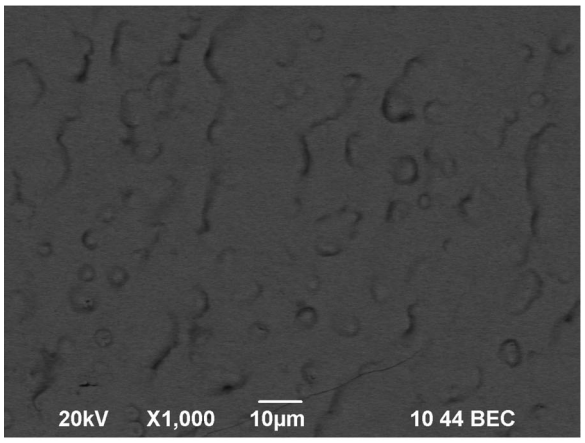

c

Figure 8. SEM of the alloy coating Zn–Cr with 9.4% Cr 'as deposited' (a) and after annealing at 220°C (b) or at 300°C (c).

maxima are seen. One of them is located just over 74°C and it is related to δ-(Zn, Fe) phase. The other maximum is located just over 78° and is due to the Γ-(Zn, Fe) phase. In the case of the alloy with 3.6 mass % Cr, these maxima are similar. At 5.4 mass % Cr in the alloy, the maxima continue to occur. However, the diffractogram of the alloy with 9.4 mass % Cr does not contain any maxima. This is understandable, since with the increase of Cr content in the alloy, a larger amount of Zn is bound in ζ-$CrZn_{13}$ phase formation and subsequently, less Zn is available for interaction with the steel substrate.

Modification of the morphology of the alloy coatings as a result of their thermal treatment

The next three figures show the morphology of samples before and after annealing at two temperatures. Figure 6 presents the modifications that occur with the samples containing 3.6 mass % Cr. Formations that look like the start of dendrites are observed on the surface of the unheated samples (Figure 6(a)). These formations contain a lower amount of Cr (about 2 mass %) compared to the base coating and a higher amount of carbon (up to about 9 mass %). After annealing at 180°C the number and the size of the formations increase, which is characteristic of oxidation processes. The Zn content decreases, while Cr is not detected. A similar result is seen in the case of alloy coatings containing 5.4 mass % Cr (Figure 7). However, the effect is not as pronounced and the formations still contain Cr. The situation becomes different in the case of alloy coatings with 9.4 mass % Cr (Figure 8). Upon heat treatment, only single formations are observed. They have slightly increased the content of C and O relative to the base surface.

Conclusions

DSC and XRD analyses are used to understand the effect of annealing temperature on phase transitions in electrodeposited Zn–Cr alloy coatings containing 3.6, 5.4 or 9.4 mass % Cr. The 'as prepared' coatings consist of the η-(Zn, Cr) phase. An increase of the Cr content leads to a decrease of the lattice parameters. Upon annealing of all three alloys, an irreversible transition to ζ-$CrZn_{13}$ phase is recorded. By increasing Cr content, the beginning of the transition shifts to higher temperatures (from 180 to 250°C). In the alloy with least Cr content, the η-(Zn) phase predominates, while in the alloy containing 9.4 mass % Cr, XRD lines of Cr also appear. The Zn–Cr alloy coating containing 5.4 mass % Cr transforms into ζ-$CrZn_{13}$ phase with traces of η-(Zn) phase. Therefore, by annealing Zn–Cr coating with a slightly higher Cr content (about 5.7 mass % Cr), only ζ-$CrZn_{13}$ phase could be obtained. The ζ-$CrZn_{13}$ phase would be suitable for use as corrosion-protective coating and warrants further investigation of the corrosion-electrochemical behaviour.

In the annealing process, the coatings interact with the steel substrate. The unalloyed Zn coating shows the strongest interaction as shown by the formation of δ-(Zn, Fe) phase and Γ-(Zn, Fe) phase. With an increase in Cr content in the alloy, such interactions become weaker. Correspondingly, no Zn–Fe phases are seen in the alloy with 9.4% Cr.

Acknowledgement

The authors would like to thank voestalpine Stahl GmbH, Linz, Austria for providing samples used in the present investigations.

Disclosure statement

No potential conflict of interest was reported by the authors.

Funding

This work was supported by the Austrian Science Foundation FFG and the government of Lower Austria and Upper Austria in the frame of the COMET-program: [grant number CEST SP 190100]. The authors acknowledge the financial support of Project BG 051PO001-3.3.06-0038.

References

[1] Steck T, Gerdenitsch J, Tomandl A, et al. Zinc-chromium coated steel sheet: properties and production. Proceedings of the 8th International Conference on Zinc and Zinc Alloy Coated Steel Sheet Galvatech; 2011 June 21–24; Genova, Italy.

[2] Luckeneder G, Fleischanderl M, Steck T, et al. Corrosion mechanisms and cosmetic corrosion aspects of zinc–aluminium–magnesium and zinc–chromium alloy coated steel strip. Proceedings of the 8th International Conference on Zinc and Zinc Alloy Coated Steel Sheet Galvatech; 2011 June 21–24; Genova, Italy.

[3] Hansen M, Anderko E. Constitution of binary alloys. Moscow: Metallurgizdat; 1962.

[4] Le Chaterier H. On the scheme of determination of metallic alloys. Comp Rend Acad Sci. 1895;120:835–837.

[5] Hartmann H, Hofmann W, Müller D. Contribution to the knowledge of zinc–chromium system. Abhandl Braunschweig Wiss Ges. 1955;7:100–106.

[6] Brown PJ. The structure of the ζ-phase in the transition metal-zinc alloy systems. Acta Cryst. 1962;15:608–612.

[7] Nakamaru H, Fujimura T, Ohnuma H, et al. Inventors; Kawasaki Steel Corporation, assignee. Corrosion resistant steel sheets improved in corrosion resistance and other characteristics. United States Patent US 5,510,196. 1996 Apr 23.

[8] Guzman L, Adami M, Gissler W, et al. Vapour deposited Zn–Cr alloy coatings for enhanced manufacturing and corrosion resistance of steel sheets. Surf Coat Technol. 2000;125:218–222.

[9] Scott C, Olier C, Lamande A, et al. Structural evolution of co-deposited Zn–Cr coatings produced by vacuum evaporation. Thin Solid Films. 2003;436:232–237.

[10] Miyake M, Hirato T, Matsubara E, et al. Structure of Zn–Cr alloy electrodeposited on steel at high current densities. Second International Conference on Processing Materials for Properties, San Francisco, California, November 5–8; 2000. p. 779–782.

[11] Hashimoto S, Ando S, Urakawa T, et al. Crystal structure of electrodeposited Zn–Cr coatings. J Japan Inst Metals. 1998;52(1):9–14.

[12] Boiadjieva T, Petrov K, Kronberger H, et al. Composition of electrodeposited Zn–Cr alloy coatings and phase transformations induced by thermal treatment. J Alloys Compd. 2009;480:259–264.

[13] Chakarova V, Boiadjieva-Scherzer T, Kovacheva D, et al. Corrosion behaviour of electrodeposited Zn–Cr alloy coatings. Corr Sci. 2018;140:73–78.

[14] Kraus W, Nolze G. PowderCell for Windows, version 2.4, Federal Institute for Materials Research and Testing, Rudower Chaussee 5, 12489 Berlin, Germany.

[15] Wienströer S, Fransen M, Mittelstädt H, et al. Zinc/iron phase transformation studies on galvannealed steel coatings by X-ray diffraction. International Centre for Diffraction Data 2003, Advances in X-ray Analysys, Volume 46, 291–296.